Transient behaviour of a suction caisson in sand : axisymmetric numerical modelling

B. Cerfontaine[1] , F. Collin[2] , R. Charlier[2]

[1] *Université de Liège, Allée de la découverte, 9, Liège, b.cerfontaine@ulg.ac.be*

[2] *Université de Liège, Allée de la découverte, 9, Liège*

...

RÉSUMÉ. *Cet article traite le problèmes des caissons à succion installés dans du sable soumis à un chargement vertical monotone et cyclique. La modélisation numérique d'un caisson en acier à l'aide du code aux éléments finis LAGAMINE est présentée par la suite. Le modèle de Prevost est utilisé pour reproduire le comportement cyclique du sol, i.e. il est capable de modéliser l'accumulation de déformation et de pressions d'eau cycle après cycle. Des éléments finis d'interface sont utilisés afin de modéliser le comportement en traction du caisson dans des conditions drainées et non drainées.*

Quel que soit le mode de chargement, le caisson présente plusieurs modes de résistance : le frottement le long du fût du caisson, la capacité portante sous la pointe et un effet de succion. La première partie de ce travail montre la mobilisation progressive de ces différents modes de résistance sous chargement monotone. Les simulations partiellement drainées sont particulièrement intéressantes car elles montrent clairement l'augmentation significative de la résistance transitoire du caisson grâce au phénomène de consolidation induit par le chargement. La seconde partie de l'article illustre l'évolution du tassement sous le caisson sous différents types de chargement.

ABSTRACT. *This paper deals with the axisymmetric behaviour of a suction caisson installed in sand upon vertical monotonic and cyclic loading. A steel caisson is numerically modelled using the finite element code LAGAMINE. The Prevost model reproduces the cyclic behaviour of the soil, i.e. it captures the accumulation of deformation and pore water pressure within the soil. Coupled interface finite elements allow the modelling of the uplift behaviour of the caisson in both drained and partially drained conditions.*

Upon compression or traction loading, the suction caisson presents different modes of resistance: friction along the shaft, bearing capacity under the lid or the tip of the caisson, suction effect. The first part of this work describes the progressive mobilisation of these modes of resistance during monotonic simulations. The partially drained effect is particularly interesting since it drastically increases the resistance to transient loading. It proceeds from the transient consolidation process induced by the caisson's loading. The second part describes the evolution of the settlement of the suction caisson upon different kind of cyclic loading signals.

MOTS-CLÉS : *Ingénierie Offshore, Caisson à succion, Sable, Modélisation Numérique*

KEYWORDS: *Offshore Engineering, Suction Caisson, Sand, Numerical modelling*

1. Introduction

Offshore wind energy is a keystone in the struggle against global warming and the total offshore capacity is strongly increasing. Foundation design is a crucial issue to ensure economic viability of offshore projects and may represent up to one third of their total cost. Therefore there is a real need of innovative foundation techniques and design procedures.

Among different types of foundations, suction caissons, also termed bucket foundations or suction anchors should be highlighted [BYR 02]. They consist of a hollow cylinder open towards the bottom. Their top (the lid) can be a stiffer plate or a dome. Installation of suction caissons is straightforward and does not require heavy equipment. Initially the caisson penetrates the seabed under its own weight. Water trapped inside is allowed to escape through an opening. It is pumped out afterwards, creating a differential of fluid pressure between inside and outside as shown in Figure 1. This differential of pressure digs the caisson into the soil [SEN 09].

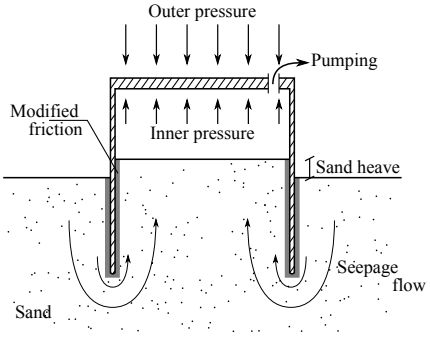

Figure 1 – Sketch of the installation process

The foundation type may be monopod or multipod. In the first case, there is a single foundation per wind turbine subjected to a combination of horizontal and overturning moment [ACH 13]. In the second, the superstructure lies on a system of foundations. The large overturning moment is mainly transformed into a push-pull loading of the suction caissons [SEN 09]. Therefore the behaviour of the caisson under large extraction load is one of the main issues [HOU 05].

The cyclic nature of the loading complicates the problem since the behaviour of sand in this case is quite complex. It is widely studied in the fields of earthquake and offshore geotechnics. The main outcome is the pore water pressure (PWP) and settlement accumulations with increasing number of cycles. This general behaviour is also observed for suction caissons experimentally [KEL 06] and numerically [CER 15a]. Therefore the modelling of this sand behaviour requires specific constitutive laws.

This paper presents numerical drained and partially drained simulations of monotonic and cyclic loadings of a suction caisson embedded in dense sand upon vertical loading. The first objective is the deep understanding of the different mechanisms of resistance of the caisson upon monotonic loading and their interactions. The second objective is to understand the cyclic behaviour of suction caissons in the light of their monotonic response.

2. Numerical model

2.1. *Geometry*

A sketch of the investigated suction caisson is provided in Figure 2a. The studied behaviour is purely vertical then the mesh is axisymmetric. The cross section of the caisson is assumed circular. The diameter D of the caisson is equal to 7.8m and its length L to 4m. The caisson is made of a stiff lid (0.4m thick), closing its upper aperture, and a more flexible skirt (0.1m thick).

The behaviour of sands is inherently non-linear and involves plasticity effects such as contractancy and dilatancy. Therefore elastic models are not sufficient. Classical elasto-plastic models are able to reproduce the monotonic behaviour of sands but not the cyclic one, involving plasticity during loading and unloading. The Prevost model is adopted in the following [CER 14]. This model is made of a yield and an arbitrary number of hardening surfaces discretising the field of hardening moduli. It takes into account the phase transition. The evolution of the stiffness parameters with confinement (p') is introduced.

A full description of the model implementation into the finite element code `LAGAMINE` and calibration of parameters can be found in [CER 14]. These parameters correspond to a very dense Lund sand [IBS 96]. The phase

transition line slope $\bar{\eta}$ is equal to 1.15 and a cohesion shift p_c to 5kPa.

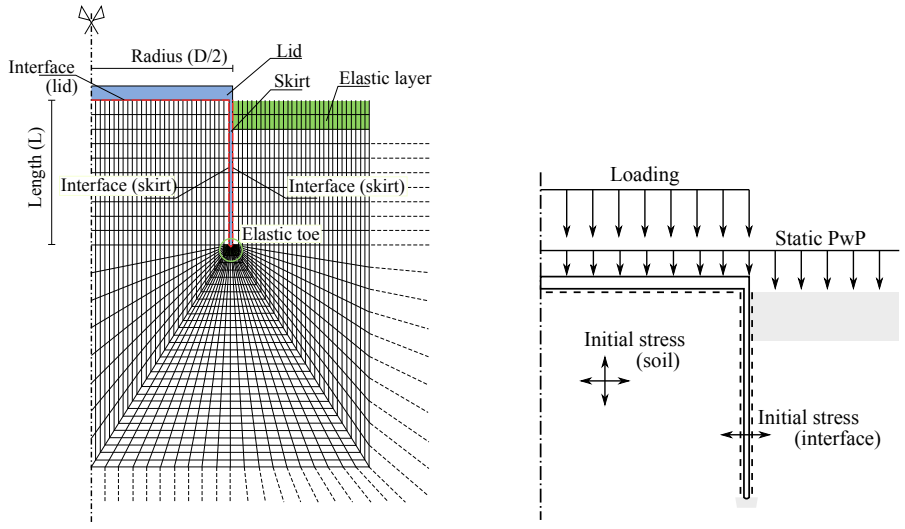

(a) Zoom on the mesh adopted around the caisson

(b) Sketch of the loading applied to the caisson and initial stresses

Figure 2

The superficial sand layer outside the caisson is prone to liquefaction due to its low confinement. However modelling its post-liquefaction is meaningless in the scope of this study since it does not contribute significantly to the resistance of the foundation. It is modelled by a linear elastic soil layer $(E, \nu) = (10\text{MPa}, 0.15)$. The depth of this layer is limited to 0.8m. It includes the first two rows of elements. Similarly an elastic toe is also set up under the tip of the caisson as shown in Figure 2a. It compensates the overestimated width of the skirt. A detailed justification of this approximation can be found in [CER 15a].
The soil is assumed to be a very dense sand (relative density of 90 %). The specific weight of the solid grains is equal to 26.5kN/m^3, the porosity of the soil to 0.36 and its permeability to $5 \cdot 10^{-12}$m^2 (corresponding to $5 \cdot 10^{-5}$m/s) [AND 08]. The caisson is made of steel and assumed to remain elastic-linear. Its parameters are equal to $(E, \nu) = (200\text{GPa}, 0.3)$.
The 26mx24m mesh is composed of 2364 hydro-mechanical coupled finite elements and 7085 nodes. Hydro-mechanical interface elements are set up between the soil and the caisson. The installation phase of the suction caisson is not considered.

2.2. *Boundary conditions and initial stresses*

The lower limit of the mesh is deemed impervious, *i.e.* it corresponds to a layer of consolidated clay under the sand layer for example. The right and upper sides of the mesh are considered drained. They respectively correspond to the continuity of the sand layer and to the transition between the sand layer and the sea. The total mesh has the size 26m $\times$ 24m. The lateral displacement is set to zero on the vertical boundary while the vertical is imposed to zero on the lower boundary.
The sea level is considered to be 10m over the sand layer. It is taken into account by a vertical pressure of 100kPa applied at the top of the soil, as represented in Figure 2b. The corresponding initial pore water pressures (PWP) are set up accordingly in the whole domain. Effective stresses are initialised within the soil (and the interface), due to its self weight. The coefficient of earth pressure at rest K_0 is assumed equal to 1. The caisson is considered already in place, so disturbances due to its installation are not taken into account.

2.3. *Loading of the caisson*

The loading of the caisson consists of a stress-controlled signal applied at the top of the lid, as shown in Figure 2b. Monotonic loading is simply a positive (compression) or negative (traction) pressure applied uniformly at a constant rate. The cyclic loading is a more complex pressure signal and is described in the following.

2.4. *Interface elements*

The accurate modelling of suction caissons necessitates the use of hydro-mechanical coupled finite elements of interface. From a mechanical point of view, the soil-caisson shearing along the skirt is important especially in traction. In compression, the top of the caisson is in contact with the soil but this contact may be lost during the simulation and soil-caisson tractions can not exist. From the hydraulic point of view, the evolution of the PWP along the walls of the caisson modifies the maximum shearing available. Moreover the opening of a gap along the skirt introduces preferential paths for water flows. The interface element is extensively described in [CER 15b]
The mechanical contact is enforced through a penalty method such that

$$\dot{\mathrm{p}}'_N = -\mathrm{K}_N \, \dot{\mathrm{g}}_N, \qquad [1]$$

where $\dot{\mathrm{p}}'_N$ is variation of effective contact pressure, K_N a penalty coefficient (equal to 10^{10} N/m^3) and $\dot{\mathrm{g}}_N$ the variation of the distance between two sides of the interface. The effective contact pressure is obtained from the following relation

$$\mathrm{p}'_N = \mathrm{p}_N - \mathrm{p}_w, \qquad [2]$$

where p_N is the total pressure at the soil-caisson interface and p_w is the water pressure. The maximum shearing resistance is bounded by

$$\tau_{max} = \mu \, \mathrm{p}'_N, \qquad [3]$$

where μ is the friction coefficient, equal to 0.5. When this maximum shear stress is reached, there is a free relative tangential displacement between the two sides of the interface.

3. Monotonic loading

Two configurations of monotonic loading are considered : drained and partially drained. In the former, the loading rate is assumed very slow with respect to the PWP dissipation rate within the soil. Therefore the PWP are constant. In the second case, PWP generated diverge from their initial value. However the simulation is not undrained and they are able to dissipate progressively.

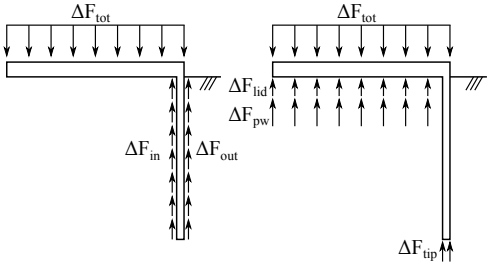

Figure 3 – Comparison of reaction components : Compression load $\Delta\mathrm{F}_{tot}$

A positive or negative variation of vertical load applied to the caisson is balanced by different components of reaction, described in Figure 3 in case of compression. The variation of total load applied on the upper part of the lid of the caisson is termed $\Delta\mathrm{F}_{tot}$. The integral of the variation of PWP distribution on the lower part of the lid of the caisson is represented by $\Delta\mathrm{F}_{pw}$. The integral of the effective normal contact stresses on this lower part are gathered into $\Delta\mathrm{F}_{lid}$. The integral of the variation of shear stresses along the skirt of the caisson is denoted $\Delta\mathrm{F}_{in}$ inside and $\Delta\mathrm{F}_{out}$ outside. In the following they are depicted with respect to the displacement of the top center of the caisson $\Delta\mathrm{y}$.
Stress-controlled simulations are carried out up to the local failure of a material point or to the global failure of the soil-caisson system. The post-failure behaviour of the system of foundations is not represented. Thence the maximum displacement remains limited.

3.1. *Compression simulations*

3.1.1. *Drained configuration*

Drained results upon compression load are provided in Figure 4a . The simulation underlines the sequential mobilisation of the reaction components. Up to 4mm of settlement, the main part of the total load ΔF_{tot} applied to the caisson is sustained by the shearing that develops along the sides of the caisson. However shear stresses within the interface progressively reach their maximum value.
Friction is not mobilised simultaneously on both sides of the skirt. Indeed, the soil-caisson relative displacement is lower inside since the soil settles with the caisson as depicted in Figure 4b. This is due to the effect of the load transferred by the lid of the caisson and the shear mobilised depends on the soil-caisson relative displacement. Another consequence is the increasing confinement of the soil inside. Therefore the ΔF_{out} component firstly reaches its maximum value but this latter increases due to the increasing confinement. Finally, further increments of total load applied are reported mainly under the lid and the tip of the caisson.

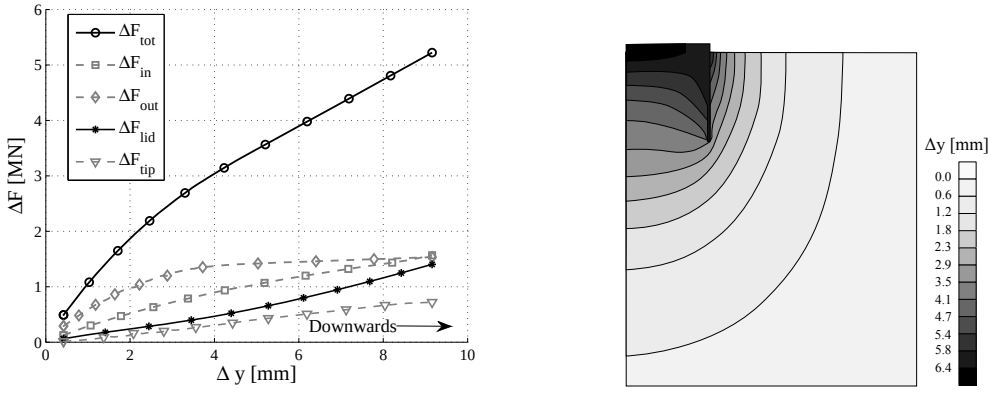

(a) Variations of global reaction components

(b) Settlement for ΔF_{tot} =4.3MN

Figure 4 – Drained compression simulation

3.1.2. *Partially drained configuration*

A partially drained compression simulation is illustrated in Figure 5. The total load is increased up to 4.3 MN at a rate of 0.4 MN/s and kept constant afterwards.
The soil-caisson system is much stiffer in partially drained than in drained conditions. The displacement required to reach the same load is almost half in the partially drained simulation. This is due to the new component of reaction induced by the PWP generation ΔF_{pw}. The loading compression of the suction caisson is nothing but a classical consolidation process. Variations of PWP are "trapped" inside the caisson due to its skirt, limiting their dissipation. The variation of the field of PWP generated within the soil upon a compression load is illustrated in Figure 6b. The difference of pressure between inside the caisson and outside it is at the origin of ΔF_{pw}.

During the compression phase, the outer shearing ΔF_{out} and suction ΔF_{pw} are the main contributors to the resistance of the caisson as depicted in Figure 5. Indeed, the PWP inside are not yet dissipated and the behaviour is almost undrained. Therefore there is nearly no effective stresses transferred by the lid to the soil and the relative displacement between the soil and the skirt is almost null inside as shown in Figure 6a. The increasing of tip ΔF_{tip}, lid ΔF_{lid} and inside shearing ΔF_{in} components is delayed when the early generated PWP dissipate.
At the end of the pushing phase, the PWP have time to dissipate and the settlement increases while the total load is kept constant. The load sustained by ΔF_{pw} is transferred to the other components of resistance. The normal effective stress within the interface also increases du to the drainage process. Therefore the maximum value of shearing components also increases. This illustrates that the increase in stiffness and resistance is a purely transient effect.

3.2. *Traction simulations*

In Figure 7a, the pull drained simulation illustrates that only the two components of friction ΔF_{in} and ΔF_{out}, actively contribute to the resistance to traction. The variation of ΔF_{tip} is only due to the deconfinement of initial

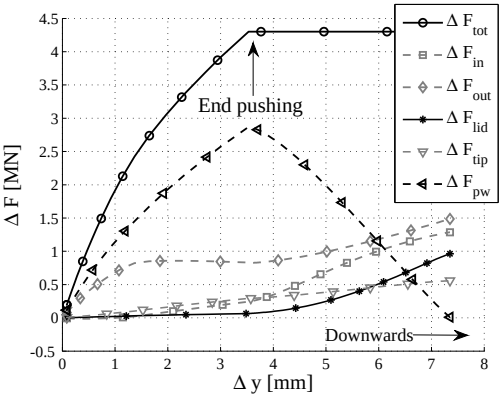

Figure 5 – Partially drained compression simulation, k= $5 \cdot 10^{-12}$m^2, rate of loading 0.4MN/s : Variations of global reaction components

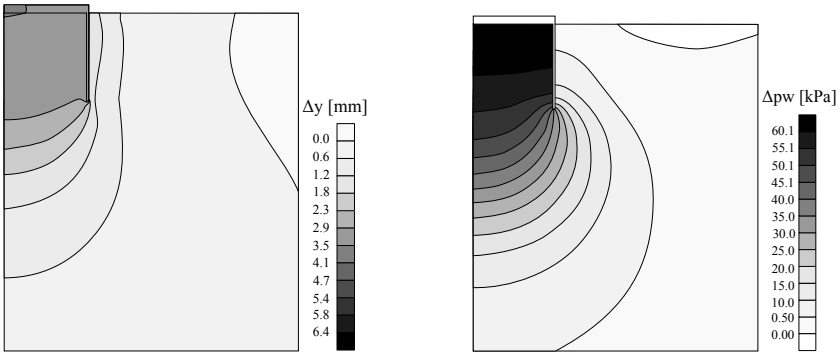

(a) Settlement of the caisson

(b) Variation of the pore water pressure

Figure 6 – Partially drained simulation, ΔF_{tot} =4.3MN, k= $5 \cdot 10^{-12}$m^2, rate of loading 0.4MN/s

stresses and does not play an active role in the resistance. The contact is lost under the lid and effective traction stresses are not admissible. Therefore the lid component ΔF_{lid} is equal to zero.
The difference of stiffness between inner and outer friction components proceeds from the uplifting movement of the soil inside the caisson. The relative soil-caisson displacement is reduced and so is the shear stress mobilisation. The outer friction is fully mobilised after an upward movement of 1.5mm and a plateau is reached in Figure 7a. Therefore the increasing load is sustained only by the mobilisation of shear stress within the inner interface. Simulation stops when it is fully mobilised and no additional load can be sustained.

The partially drained simulation depicted in Figure 7b illustrates the increase of resistance obtained by considering the fluid flow surrounding the caisson. Indeed, if the loading rate of the caisson is equal to 0.4MN/s, the total load sustained for a displacement of -1.5mm is increased by almost 50%. This phenomenon is supported by experimental [BYR 02] and numerical [THI 14] evidences. The negative variations of fluid pressure increase the normal effective stress within the soil-caisson interface and then the maximum friction available. The absolute value of ΔF_{out} is slightly greater than in drained conditions.

3.3. *Influence of soil's permeability in traction*

It was shown that the suction component can significantly increase the total resistance to traction load. Permeability of the soil and rate of loading both modify the available suction. Traction simulations for three order of magnitudes of permeability are illustrated in Figure 8.
The stiffness of the soil-caisson system increases with decreasing permeability of the soil. Indeed, the negative PWP inside the caisson are less rapidly dissipated, maintaining a high differential of pressure. However the corollary effect is the generation of high pressure gradients leading to local liquefaction of the soil.

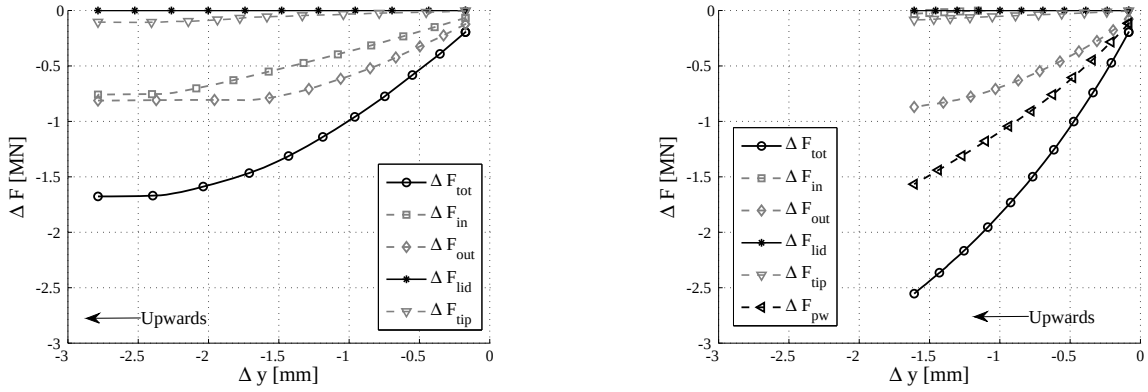

(a) Drained

(b) Partially drained, rate of loading 0.4MN/s

Figure 7 – Traction simulation, variations of global reaction components

For a similar applied traction load, the uplift displacement of the caisson also increases with increasing permeability. For the highest permeability, there are clearly two distinct phases. During the first phase (down to almost -1.5mm), the stiffness of the caisson is only slightly different from the other simulations. This corresponds to the progressive mobilisation of friction along the caisson's walls (inside and outside). After this point, the stiffness suddenly degrades. This actually corresponds to the full mobilisation of friction on the skirt inside and outside the caisson. The caisson slides upwards and suction $\Delta \mathrm{F}_{pw}$ is the only component of resistance. In this case, there is also a loss of contact between the lid and the soil, creating a gap. This gap is filled with water and the caisson acts like a piston.

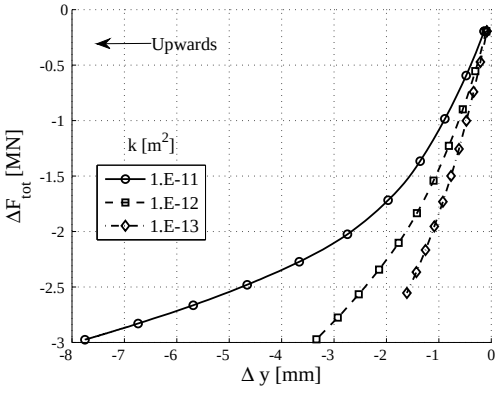

Figure 8 – Influence of the permeability on partially drained results, pull rate 0.4MN/s

4. Cyclic loading

4.1. *Loading*

The cyclic load is applied in three phases. The first consists in applying monotonically a mean load $\mathrm{p}_{tot,mean} = 20$kPa, in a drained fashion. This load corresponds to the weight of the wind turbine and the constant component of the storm. The second phase is the application of a cyclic loading around the mean load. Finally a 300s consolidation phase at constant initial mean load is simulated in order to allow dissipation of PWP and to compute a final settlement.

The cyclic loading of the caisson originates from the effects of wind and waves acting on the offshore superstructure. A typical output of the analysis of a tripod superstructure to waves and wind is presented in Figure 10a (top figure). It is termed pseudo-random since it results from a numerical analysis by specialised software. It corresponds to a storm sample including an extreme event, *i.e.* the biggest load encountered by the superstructure during the storm. Only the vertical load applied by a leg of the superstructure is considered.

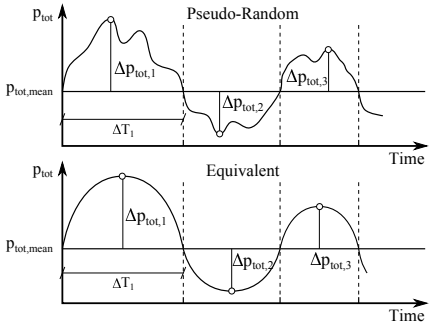

Figure 9 – Half-cycle analysis of the load signal p_{tot}

Within the pseudo-random signal, high amplitude cycles alternate with the low amplitude ones and the effect of each type of cycle is difficult to isolate. A half-cycle analysis [BYR 02] is carried out to transform the pseudo-random signal into a sinusoidal equivalent one. A half-cycle is defined as the part of a signal between two successive crossings of its mean value, as shown in Figure 9. A half period $\Delta\mathrm{T}$ and a peak value $\Delta\mathrm{p}_{tot}$ are associated to each half-cycle. Therefore an equivalent sinusoidal cycle of identical characteristics ($\Delta\mathrm{T}$,$\Delta\mathrm{p}_{tot}$) can be reconstituted.
In this study, four types A_i of periods and amplitudes are identified in the pseudo-random load signal. They are supplied in Table 1. For each category A_i, N_i cycles are identified in the pseudo-random signal. These equivalent cycles are ordered into equivalent load signals, as depicted in Figure 10a. These signals mainly differ by the position of the extreme event, at the beginning, in the middle or at the end. A more detailed description of the method could be found in [CER 14].

	A1	A2	A3	A4
Number of cycles [-]	50	28	4	1
$\Delta\mathrm{p}_{\mathrm{tot}}$ [kPa]	4.5	13.5	22.5	40.5
T [s]	4.6	11	11.6	11.1

Tableau 1 – Number of equivalent cycles, associated amplitudes and periods

4.2. *Results*

Figure 10b presents a comparison between the first equivalent and the pseudo-random load signals. The variation of the total load $\Delta\mathrm{p}_{tot}$ around its mean value $\mathrm{p}_{tot,mean}$ is represented as well as the averaged PWP under the lid of the caisson $\Delta\mathrm{p}_w$. The full response signal is difficult to analyse due to the large number of cycles. Therefore the envelope curve, i.e. the locus of local minima or maxima is represented for both $\Delta\mathrm{p}_{tot}$ and $\Delta\mathrm{p}_w$.
The tendency curve describes the long-term evolution of the PWP. If the process was totally reversible, the PWP should be equal to zero each time the cyclic amplitude Δp_{tot} is equal to zero. However $\Delta\mathrm{p}_w$ is not equal to zero, denoting a non recoverable part. The locus of all these non-recoverable parts describes the tendency response in Figure 10b.
It can be observed that the variation of PWP insidde the caisson $\Delta\mathrm{p}_w$ is almost identical to the variation of the total load applied $\Delta\mathrm{p}_{tot}$. This is a consequence of the partially drained behaviour highlighted for monotonic simulations. A large part of the loading is sustained by a PWP variation which is hardly dissipated before the load reverses. Therefore the cyclic effective amplitude applied to the solid skeleton of the soil surrounding the caisson is much lower than the total cyclic amplitude applied on the caisson. Consequently this partially drained behaviour induces less stiffness degradation and settlement than a drained behaviour.
Both response signals present a tendency to PWP accumulation. Such an observation is classical in undrained laboratory experiments on soil samples [SEE 66] or in offshore engineering in general [CUE 14]. This results from the plasticity of the soil, implying excess PWP in partially drained conditions. In the upper graph of Figure 10b, it can be observed that a maximum accumulation arises after the extreme event. It is progressively dissipated afterwards during cycles of lower amplitudes.

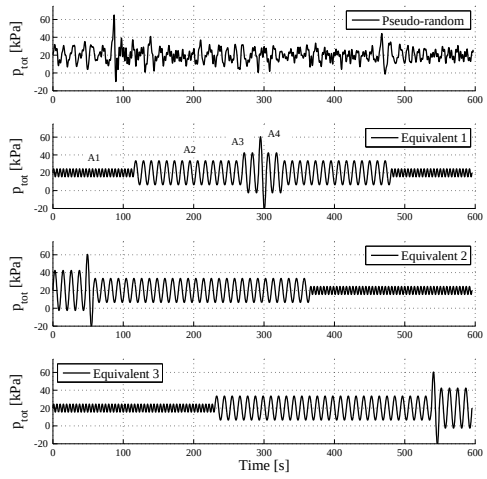

(a) Pseudo-random and equivalent cyclic load signals

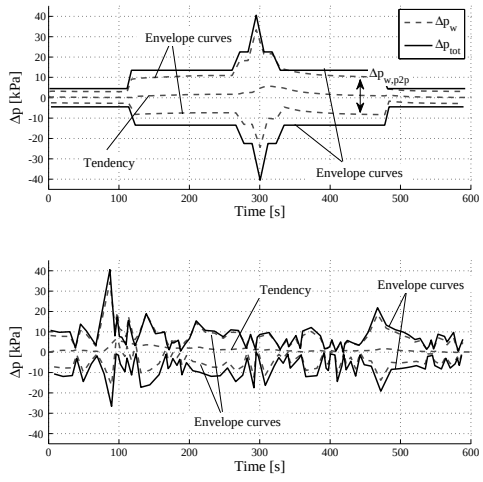

(b) Comparison of cyclic variation of total pressure applied on the lid Δp_{tot} and variation of mean pore pressure inside the caisson Δp_w for two load signals : Equivalent 1 (up) and pseudo-random (down)

Figure 10

The cyclic loading of suction caissons can be decomposed into two parallel consolidation processes. The first, *named short-term*, consists of the immediate response of the soil to the variation of the applied load at the scale of a cycle. Variations of PWP are large since the load reverses before all PWP are dissipated. It is the origin of the "suction effect". The displacement varies accordingly and is mainly recoverable.
On the contrary the second consolidation process arises from the progressive dissipation of the accumulated PWP and is termed *long-term*. It results from the plastic contractancy of the soil and is responsible of the non-recoverable settlement. Accumulation of deformation during cyclic loading is also a classical results since it is linked to the accumulation of PWP.
The trend of settlement accumulation is computed similarly to the trend of PWP. It is the locus of the settlements measured each time the total load applied is equal to its mean value. Only this trend is represented since the full response signal is illegible due to the large number of cycles. The evolution of this permanent settlement under the top centre of the caisson is represented in Figure 11. The maximum transient settlement encountered during the storm event (the global maximum) is also represented since it could affect serviceability.
Results presented converge to a similar final settlement, justifying the pertinence of the half-cycle analysis method for the elaboration of a load signal. However there is a small divergence between them since the stress paths of material points are not identical for all load signals.
One of the advantages of such a load signal is the clarification of the effect of each type of cycles (A1,A2,A3 or A4). The low-amplitude cycles lead to almost no plastic deformation. This is quite clear in results corresponding to Equiv. 3 load signal but totally impossible to observe in the pseudo-random response. The second batch of cycles (A2) exhibits a clear tendency of settlement accumulation which could be extrapolated to a larger number of cycles. The asymptotic non-linear evolution of the settlement is due to the progressive dissipation of the accumulated PWP, which is maximum during the extreme event. Therefore the sooner this event occurs, the sooner this asymptotic evolution starts.

5. Conclusions

Suction caissons represent an interesting competitive alternative to other types of foundations for offshore wind turbines. However their behaviour upon traction and cyclic loading is not entirely mastered and simplified methods for design should still be elaborated. This paper presents the results of monotonic and cyclic loading of a suction caisson embedded in dense sand.
Upon traction, the main mechanism of reaction is the friction progressively mobilised along the skirt of the caisson. It is mobilised inside and outside the caisson in drained conditions (low pull rate). Upon high rate of loading, a

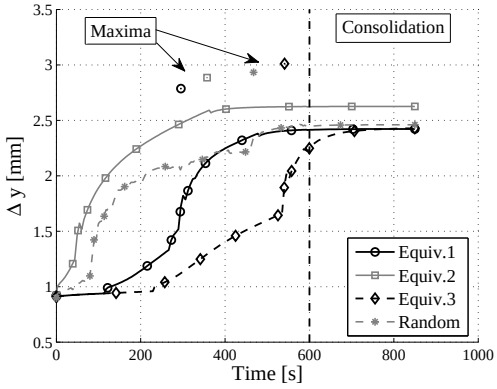

Figure 11 – Evolution of the permanent displacement for four load signals (equivalent 1, equivalent 2, equivalent 3 and pseudo random)

consolidation process takes place, generating over- or under- pressures respectively with compression or traction loads. The transient differential of pressure between inside and outside the caisson creates a suction effect, increasing the resistance of the caisson in both traction and compression. It is of greater importance in traction than in compression. Permeability and loading rate strongly influence stiffness and resistance of the caisson.
The cyclic loading of suction caissons is mainly partially drained. Therefore, the major part of the load variation is sustained by positive or negative variations of PWP within the soil inside the caisson and around it. The principal consequence is a low loading of the solid skeleton of the soil. All simulations present an accumulation of settlement during the cyclic loading of the caisson, but it is reduced with respect to a purely drained behaviour.

6. Bibliographie

[ACH 13] ACHMUS M., AKDAG C. T., THIEKEN K., « Load-bearing behavior of suction bucket foundations in sand », *Applied Ocean Research*, vol. 43, p. 157–165, 2013.

[AND 08] ANDERSEN K., JOSTAD H., DYVIK R., « Penetration resistance of offshore skirted foundations and anchors in dense sand », *Journal of Geotechnical and Geoenvironmental Engineering*, vol. 134, n° 1, p. 106–116, 2008.

[BYR 02] BYRNE B., HOULSBY G., « Experimental investigations of response of suction caissons to transient vertical loading », *Journal of the Geotechnical and Geoenvironmental Engineering*, vol. 128, n° 11, p. 926–939, 2002.

[CER 14] CERFONTAINE B., The cyclic behaviour of sand, from the Prevost model to offshore geotechnics, PhD thesis, University of Liege, september 2014.

[CER 15a] CERFONTAINE B., COLLIN F., CHARLIER R., « Numerical modelling of transient cyclic vertical loading of suction caissons in sand », *Géotechnique*, vol. 65, n° 12, Thomas Telford Ltd, 2015.

[CER 15b] CERFONTAINE B., DIEUDONNE A., RADU J., COLLIN F., CHARLIER R., « 3D zero-thickness coupled interface finite element : Formulation and application », *Computers and Geotechnics*, vol. 69, p. 124–140, Elsevier, 2015.

[CUE 14] CUELLAR P., MIRA P., PASTOR M., FERNÁNDEZ MERODO J., BAESS LER M., RÜCKER W., « A numerical model for the transient analysis of offshore foundations under cyclic loading », *Computers and Geotechnics*, vol. 59, p. 75–86, juin 2014.

[HOU 05] HOULSBY G., KELLY R., BYRNE B., « The tensile capacity of suction caissons in sand under rapid loading », *Frontiers in offshore geotechnics*, p. 405–410, 2005.

[IBS 96] IBSEN L., JACOBSEN F., Lund Sand No. 0, rapport, Aalborg University, 1996.

[KEL 06] KELLY R., HOULSBY G., BYRNE B., « A comparison of field and laboratory tests of caisson foundations in sand and clay », *Géotechnique*, vol. 56, n° 9, p. 617–626, 2006.

[SEE 66] SEED B., LEE K., « Liquefaction of saturated sands during cyclic loading », *Journal of Soil Mechanics & Foundations Div*, vol. 92, 1966.

[SEN 09] SENDERS M., RANDOLPH M., « CPT-Based Method for the Installation of Suction Caissons in Sand », *Journal of Geotechnical and Geoenvironmental Engineering*, vol. 135, n° January, p. 14–25, 2009.

[THI 14] THIEKEN K., ACHMUS M., SCHRÖDER C., « On the behavior of suction buckets in sand under tensile loads », *Computers and Geotechnics*, vol. 60, p. 88–100, Elsevier Ltd, juillet 2014.